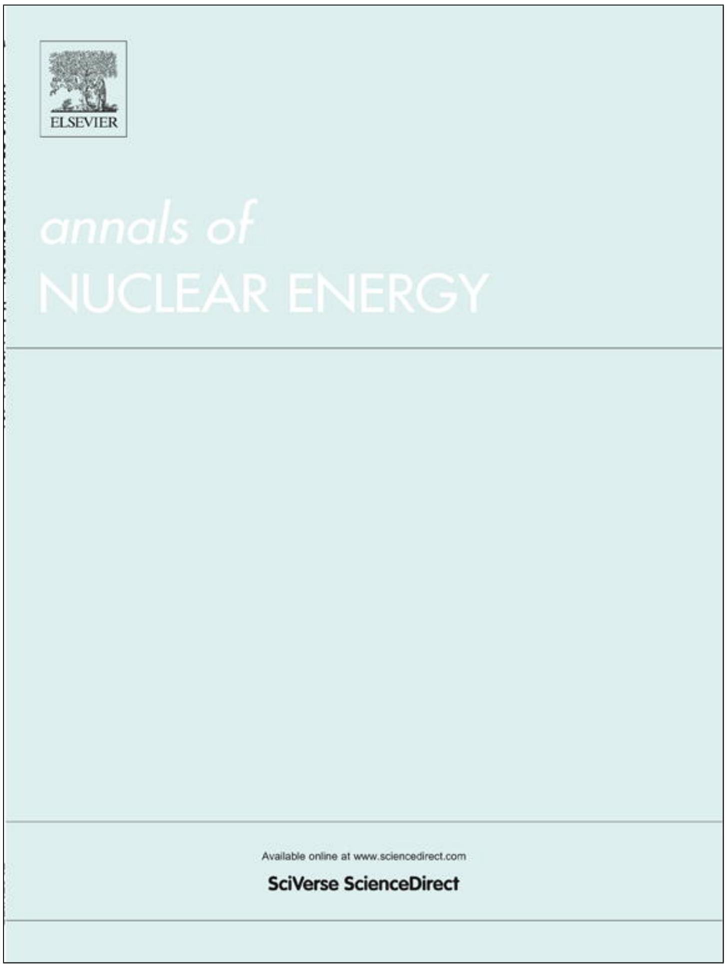
ELSEVIER
annals of
NUCLEAR ENERGY
Available online at www.sciencedirect.com
SciVerse ScienceDirect

Annals of Nuclear Energy 55 (2013) 288–291

Contents lists available at SciVerse ScienceDirect

Annals of Nuclear Energy

journal homepage: www.elsevier.com/locate/anucene

Comparison of photon attenuation coefficients of various barite concretes and lead by MCNP code, XCOM and experimental data

S.P. Shirmardi [a,*], M. Shamsaei [b], M. Naserpour [c]

[a] Nuclear Fuel Cycle Research School, Nuclear Science and Technology Research Institute (NSTRI), Tehran, Iran
[b] Faculty of Nuclear Engineering and Physics, Amir Kabir University of Technology, Tehran, Iran
[c] Faculty of Physics, Islamic Azad University, Central Tehran Branch, Tehran, Iran

ARTICLE INFO

Article history:
Received 15 October 2012
Received in revised form 17 December 2012
Accepted 1 January 2013

Keywords:
Barite
Concrete
MCNP
Linear attenuation coefficient

ABSTRACT

In this study shielding properties of various barites concretes and lead in three high gamma energies 0.662, 1.173, and 1.332 MeV were investigated using the MCNP-4C code and compared with predictions from the XCOM code and experimental data. In the three selected energies, the simulated and available data values were compared and results showed a good agreement. The results of the three methods show that lead, and pure (100%) barite have higher linear attenuation coefficients and lower transmission factors and mean free path values relative to 50% barite and 0% barite concretes.

1. Introduction

The use of X- and gamma-rays in various fields such as in radiotherapy, imaging and sterilization is increasing, however the leakage and scattering of these rays can be harmful for human-beings. Proper shielding is one of the important and necessary precautions in working with these radiations (Cember and Johnson, 2009; Chilton et al., 1984). Planning the appropriate shielding for nuclear centers depends on several factors such as the type of radiation, energy and cost. Mostly high atomic number and high density materials are used for this purpose; but the latters are costly, hence their use is limited. The exploited materials are stainless steel and lead. Concrete is more applicable material than other radiation shielding materials because of its resistance and low cost. One of the concrete types used for radiation shielding is barite.

Barite ($BaSO_4$) can be used directly or as an aggregate in concrete for shielding purposes. The shielding properties of this material against radiation are presented in terms of the linear attenuation coefficient μ (cm^{-1}) and it is defined as the probability of a radiation interacting with a material per unit path length (Woods, 1982). Previously, extensive studies on the linear attenuation coefficient of different materials have been conducted (Akkurt et al., 2009, 2010, 2012; Bashter, 1997; Dunster et al., 1971; Demir et al., 2011; Hubbell and Seltzer, 2004; Kharita et al., 2008, 2009; Medhat, 2009; Topcu, 2003). Three important gamma ray energies, 662, 1.173 and 1332 keV are considered in this work. The 662 keV gamma energies are produced from Cesium-137 which is a radioactive isotope of cesium and are utilized to calibrate nuclear detectors. It is sometimes employed in radiotherapy, medical, health and sterilization activities and it is also used industrially in gauges for measuring liquid flows and the thickness of materials. The 1173 and 1332 keV gamma energies are produced from Cobalt-60. This radionuclide is a neutron activation radioisotope product, which emits two highly penetrative gamma rays: 1173 and 1332 keV. Cobalt-60 is mainly used as a therapy agent for cancers, as a sterilizer of medical equipment, as a radiation source for radiography in industries, as a radioactive source for gauging. The mentioned numerous applications of these three gamma ray sources justify the necessity of designing and researching on the shielding properties of several types of concrete used against these radiations in nuclear and medical centers.

The aim of this study is validation of reported data on different barite concrete types and lead. Thus, some shielding parameters of barite concrete and lead measured by means of MCNP code. The MCNP results were compared with the reported experimental and XCOM results by Akkurt et al. (2010) and Medhat (2009).

2. Experimental procedures

2.1. MCNP simulation code

MCNP code is a Monte Carlo radiation transport code used for modeling the transport and the interaction of radiation with mat-

* Corresponding author. Tel./fax: +98 9126864850.
E-mail address: p_shirmardi@aut.ac.ir (S.P. Shirmardi).

0306-4549/$ - see front matter © 2013 Elsevier Ltd. All rights reserved.
http://dx.doi.org/10.1016/j.anucene.2013.01.002

ter. It utilizes the nuclear cross section libraries and uses physics models for particle interactions and gives the required quantity with certain error (Eakins, 2007; Shultis and Faw, 2010). This simulation code is used as a main tool for the implementation of this work.

2.2. Concrete and detector geometries

For implementation of geometry, the reported dimensions in Akkurt's article were employed for NaI (Tl) detector and barite concrete, so that we used the cylindrical model in MCNP cell card for them (Akkurt et al., 2010; Medhat, 2009). For investigating the variation of parameters in depth, the concrete is divided into 10 sections, a section of which has 10 cm thickness each. Multiple scattering and buildup effects were taken into account in Monte Carlo simulation code.

2.3. Gamma source

The sources were considered as planar ones with uniform distribution of radioactive material that emit gamma rays perpendicular to the front face of the shields. A disc source was defined in MCNP data card with ERG, PAR, POS, and DIR commands for energy, type of particle, position and direction respectively.

2.4. Materials specification of concrete

For specification of material in MCNP simulation, the user has to obtain the elemental composition of concrete and lead on the base of their chemical composition and weight percent. The percentages by weight of the different elements for different types of barite concrete are presented in Table 1.

Using MCNP code, barite is used in fractions of 0%, 50%, and 100% in various types concrete tagged as BC0, BC50 and BC100, respectively. Then we compare the results with available experimental values and XCOM code (Akkurt et al., 2010; Medhat, 2009).

2.5. Linear attenuation coefficient, transmission factor, mean free path

The parameters of linear attenuation coefficient, transmission factor and mean free path are calculated and compared with the results of available in literature.

The linear attenuation coefficient (μ) is defined as the fractional decrease, or attenuation of the gamma-ray beam intensity in good geometry per unit thickness of absorber, as defined by the following equation:

$$Limit\ \Delta I / I\Delta t = -\mu \quad \Delta t \rightarrow 0 \tag{1}$$

where $\Delta I/I$ is the fraction of the gamma-ray beam attenuated by an absorber of thickness Δt (Cember and Johnson, 2009). In other words, linear attenuation coefficient is defined as the probability of radiation interacting with a material per unit path length.

The transmission factors of any type of concrete, $T(E,d)$, for gamma of energy E through the thickness d (cm) of shielding the concrete was defined by dividing the absorbed dose value, $D(E,d)$, attained by the Tally F6 (F6 in MCNP code is used for calculation of particle energy deposition or kerma in material) in the dosimetric volume located behind the thickness d (cm) of the shielding to the absorbed dose value, $D(E,0)$, in the same dosimetric volume in the absence of any shielding material, as shown in the following equation:

$$T(E,d) = D(E,d)/D(E,0) \tag{2}$$

Table 1
Chemical composition of the different barite rate.

Chemical compositions	BC0 (0%barite)	BC50 (50% barite)	BC100 (100% barite)
CaO	39.394	20.269	4.794
MgO	10.970	4.925	0.648
NaO	0.394	0.175	0.027
K_2O	0.045	0.034	0.024
Fe_2O_3	0.464	0.394	0.229
P_2O_5	0.003	0.013	0.019
CO_2	31.463	12.810	0
SiO_2	12.700	7.626	3.290
H_2O	7.420	6.103	3.909
Al_2O_3	1.038	1.353	1.364
SO_2	0.460	0.378	0.205
$BaSO_4$	0	46.012	83.046
$MgCO_3$	0	0.049	0.090
NaCl	0	0.049	0.090
$CaCO_3$	0	0.998	1.801
MnO_2	0	0.099	0.180
NiO	0	0.099	0.180

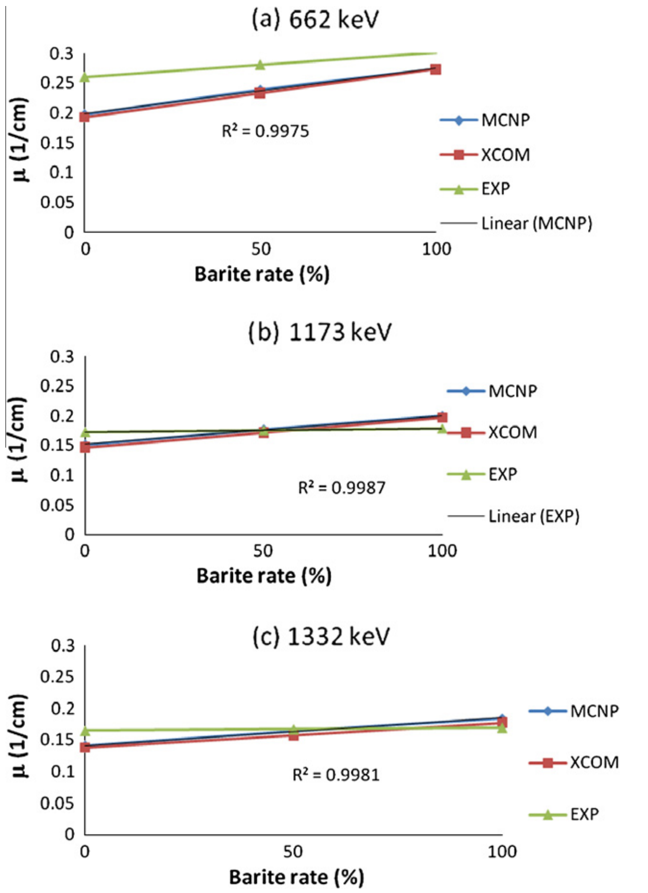

Fig. 1. Variation of the linear attenuation coefficients versus barite rates in three gamma energies (a–c).

Table 2
The photon attenuation coefficient calculated by MCNP code (with five run repetition).

Samples	Density (g/cm^3)	662 keV	1773 keV	1332 keV
BC0	2.46	0.197 ± 0.002	0.152 ± 0.001	0.141 ± 0.002
BC50	2.99	0.239 ± 0.001	0.177 ± 0.002	0.164 ± 0.002
BC100	3.463	0.274 ± 0.001	0.200 ± 0.002	0.184 ± 0.002
Pb	11.30	1.207 ± 0.001	0.694 ± 0.002	0.625 ± 0.002

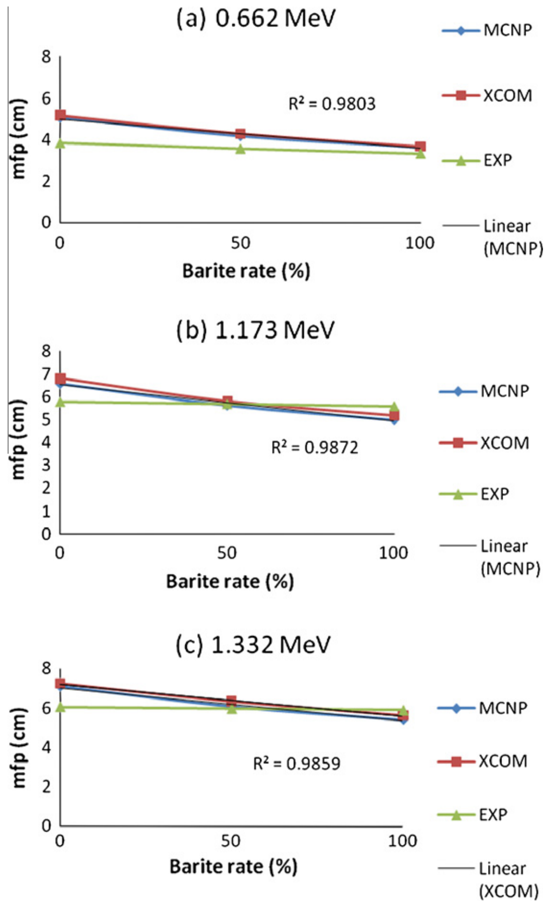

Fig. 2. Variation of the mean free path versus barite rate in three gamma energies.

Mean free path (Mfp) is defined as the average distance between the two successive interactions of photons. It is given as:

$$\mathrm{Mfp} = \frac{1}{\mu} \tag{3}$$

2.6. Relative error

For each tally, MCNP not only calculates the sample mean $\bar{x}$, but several other statistics. One of the most important is the relative error R defined as $R \equiv S\bar{x}/\bar{x}$. R generally must be less than 10% for meaningful results.

3. Results and discussion

The linear attenuation coefficients for different types of barite (0%, 50% and 100%) were calculated at three energies of 662, 1173 and 1332 keV, and the results were compared with lead and available experimental data.

Fig. 1 and Table 2 show the variations of the attenuation coefficient versus the barite rate at three gamma energies. By the comparison of the results obtained for barites with MCNP, it can be seen that the linear attenuation coefficients increased with increasing the concentration of barite in concrete. It can also be obviously seen from these figures that the linear attenuation coefficient is the highest for lead.

At low energy, the photoelectric absorption is the dominant constituent, therefore absorption is considerable, with the increase in energy, especially for the Co-60 sources in this study, the absorption is reduced, and thus the attenuation coefficient is reduced.

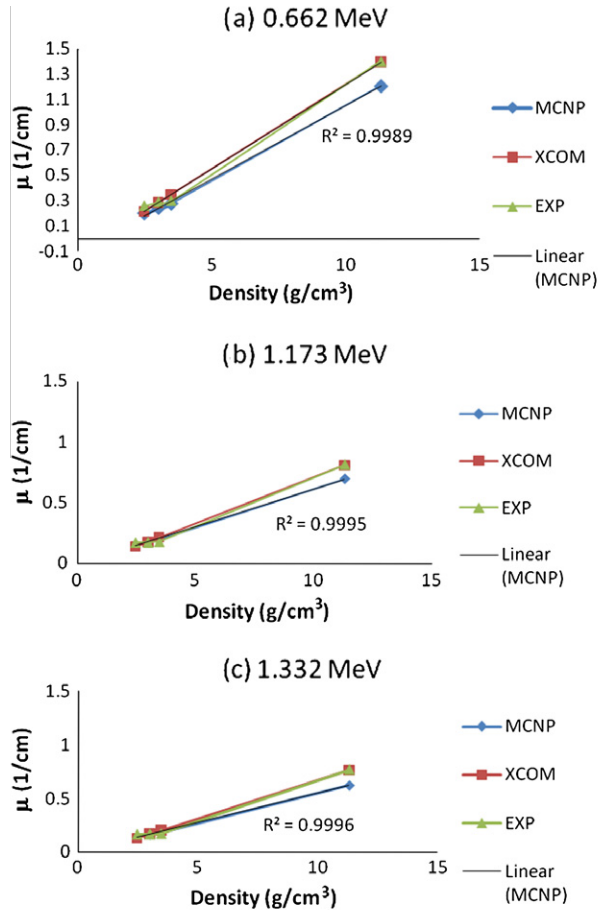

Fig. 3. Variation of the linear attenuation coefficients versus density in three gamma energies.

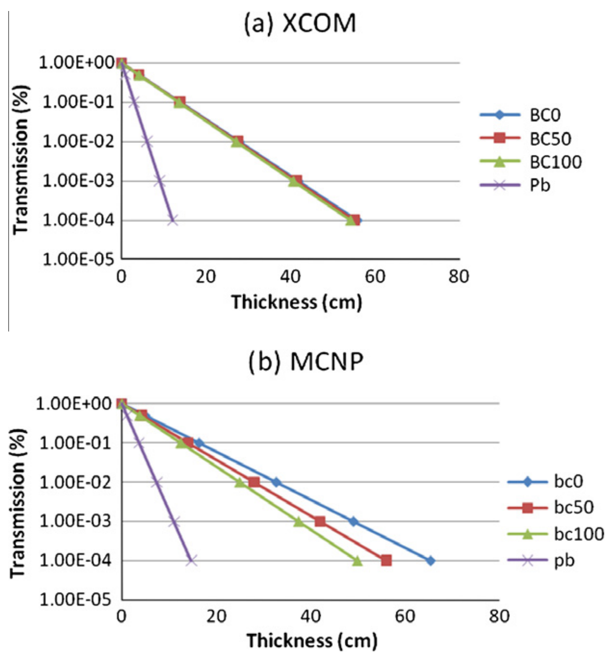

Fig. 4. The transmission rate for BC0, BC50, BC100 and lead as a function of thickness calculated by (a) XCOM and (b) MCNP code in energy 1.332 MeV.

However, increase in the barite concrete rate (increasing the percentage of high atomic number elements), will result a higher concrete density, thus leads to an increase in attenuation coefficient. It is seen from Fig. 2 that the low energy photon can deposit its energy in a short distance but high energy photons require long distances to lose their energies. It is also clear that photons deposit its energy in a short distance for a concrete containing higher barite fractions than the other types for all energy. Fig. 2 shows that the mean free path will increase with increasing the energy but decrease in high barite rate.

The linear attenuation coefficient is increased by increasing the density, as shown in Fig. 3 and Table 2. This figures show the obtained results by MCNP have more adaption in low density but there is a considerable difference in high density (in lead) that may be due to MCNP weaknesses.

The obtained results for transmission factor showed that this parameter is lower for lead and barite 100% loaded concrete than 50% barite and 0% barite bearing concrete. These results show a moderately good agreement with the reported values by Akkurt et al. (Fig. 4a and b). The differences between MCNP and experimental result can be expected from probabilistic processes or due to errors in the experimental setup. All simulation results obtained by MCNP-4C code were reported with less than 4% relative error.

4. Conclusion

In the three selected energies (662, 1173 and 1332 keV), the shielding and relevant parameters based on the elemental composition of the concrete types are simulated and in order to validate the simulation results, the available experimental data and XCOM results were compared with them. By comparing the results obtained for barites with MCNP, it can be seen that the linear attenuation coefficients increased with increasing the concentration of barite in the concrete. The mean free path will increase with increasing the energy but decrease for high barite concentrations. The obtained results for transmission factor showed that this parameter is lower for lead and pure (100%) barite concrete. The results indicated that there is a moderately good agreement between MCNP, XCOM and the experimental results. All simulation data obtained by MCNP-4C code were reported with less than 4% relative error.

Acknowledgments

The authors should like to thank Dr. Roushanzamir and Seyed Armin Shirmardi for their effective cooperation on this work.

References

Akkurt, I., Akyıldırım, H., Mavi, B., Kilincarslan, S., Basyigit, C., 2010. Photon attenuation coefficients of concrete includes barite in different rate. Ann. Nucl. Energy 37, 910–914.

Akkurt, I., Akyıldırım, H., Karipcin, F., Mavi, B., 2012. Chemical corrosion on gamma-ray attenuation properties of barite concrete. J. Saud. Chem. Soc. 16, 199–202.

Akkurt, I., Kılıncarslan, S., Basyigit, C., Mavi, B., Akyıldırım, H., 2009. Investigation of photon attenuation coefficient for pumice. Int. J. Phys. Sci. 4, 588–591.

Bashter, I.I., 1997. Calculation of radiation attenuation coefficients for shielding concretes. Ann. Nucl. Energy 24 (17), 1389–1401.

Cember, H., Johnson, E., 2009. Introduction to Health Physics Department of Environmental and Radiological Health Sciences, fourth ed. Colorado State University, Fort Collins, Colorado.

Chilton, A.B., Shultis, J.K., Faw, R.E., 1984. Principles of Radiation Shielding. Prentice-Hall, Englewood Cliffs, NJ.

Demir, F., Budak, G., Sahin, R., Karabulut, A., Oltulu, M., Un, A., 2011. Determination of radiation attenuation coefficients of heavyweight- and normal-weight concretes containing colemanite and barite for 0.663 MeV c-rays. Ann. Nucl. Energy 38, 1274–1278.

Dunster, H.J., Ellis, R.E., Jones, B.E., Jones, E.W., Rees, J.M., 1971. Handbook of Radiological Protection. Part 1: Data. Radioactive Substances Advisory Committee HMSO London.

Eakins, J., 2007. An MCNP-4C2 Determination of Gamma Source Shielding Health Protection Agency Center for Radiation, Chemical and Environmental Hazards Radiation Protection Division, ISBN 978-0-85951-603-7.

Hubbell, J.H., Seltzer, S.M., 2004. Tables of X-ray Mass Attenuation Coefficients and Mass Energy-Absorption Coefficients (Version 1.4). National Institute of Standards and Technology, Gaithersburg, MD, USA.

Kharita, M.H., Yousef, S., AlNassar, M., 2009. The effect of carbon powder addition on the properties of hematite radiation shielding concrete. Prog. Nucl. Energy 51, 388–392.

Kharita, M.H., Takeyeddin, M., Alnassar, M., Yousef, S., 2008. Development of special radiation shielding concretes using natural local materials and evaluation of their shielding characteristics. Prog. Nucl. Energy 50, 33–36.

Medhat, M.E., 2009. Gamma-ray attenuation coefficients of some building materials available in Egypt. Ann. Nucl. Energy 36 (6), 849–852.

Shultis, J.K., Faw, R.E., 2010. An MCNP Primer. Kansas State University, Department of Mechanical and Nuclear Engineering.

Topcu, I.B., 2003. Properties of heavyweight concrete produced with barite. Cem. Concr. Res. 33, 815–822.

Woods, J., 1982. Computational Methods in Reactor Shielding. Pergamon Press, New York.